The University of Osaka
Institutional Knowledge Archive

Analysis of Detection Sensitivity of Arc Sensor in Welding Process

Katsunori INOUE*, Jin-chun ZHANG**, Mum-gyu KANG***

Abstract

The detection sensitivity of an arc sensor is influenced by the wave frequency of a wire. To explain this phenomenon and to understand the characteristics of an arc sensor from theory and experiment, a simultaneous differential equation used to unstable welding state can be deduced from theoretical and experimental equations, the welding parameters (arc length, wire extension) are calculated by using this simultaneous differential equation, the results can be checked through experiment. The conclusion is that the signal is detected easily under high frequency than low frequency, because the current difference to side of groove under high frequency is bigger than low frequency.

KEY WORDS : (Arc Sensor)(MAG-Welding)(Detection Sensitivity)

1. Introduction

To promote automatization and to secure quality in welding process, seam tracking techniques have been widely used. The arc sensor is one of these. Due to the fact it does not need other units from which the signal can be directly detected from the welding arc, this type of sensors is very interesting for people in welding field. When a welding torch is waved, the physical parameters of arc's characteristics (welding current, voltage etc.) are detected so that it become obvious that the welding seam is automatically tracked.

In the welding process the detection sensitivity of an arc sensor is greatly influenced by the wave frequency of a wire. Until now this phenomenon has till not been analyzed theoretically, because the welding process using an arc sensor is carried out under the unstable conditions. Since the arc length and wire extension change with the position of the wire in the groove, it is difficult to analyze the phenomenon theoretically or experimentally.

In this paper, to analyze this phenomenon, a new method is used. A simultaneous differential equation can be deduced from theoretical and experimental equations. The results calculated by these equations are verified by the experiment. In practice some parameters (arc length, wire extension) can be not directly detected in welding process, but these parameters may be calculated by means of the equations. After the necessary parameters are calculated, it is easy to solve these problems. The calculated result show that when the wave frequency of a wire is changed, the arc self-regulation characteristic is influenced, so that the detecting sensitivity of arc sensor is also influenced.

2. Theory and Calculation

2.1 Basic formula for analysis

To calculate the physical parameters in the welding process, a mathematical model of the arc welding process is based on the analysis of the known mathematical relationships in the form of the following system of equations[1]:

$$V_0 = L \cdot dIa/dt + Ia \cdot R + Ve + Va \qquad (1)$$
$$Ve = \alpha_1 \cdot le \cdot J - \alpha_2 \cdot Vf/J \qquad (2)$$
$$Va = \beta_1 \cdot Ia + \beta_2 + (\beta_3 \cdot Ia + \beta 4) \cdot la \qquad (3)$$
$$Vm = \gamma_1 \cdot J + \gamma_2 \cdot le \cdot J^2 \qquad (4)$$
$$dle/dt = Vf - Vm \qquad (5)$$
$$J = 4 \cdot Ia/(\pi \cdot de^2) \qquad (6)$$

where
R = Ri + Rl + Rnp + Rk

Ri : Internal resistance of the welding source
Rl : Pure resistance of the throttle
Rnp : Pure resistance of the conductors
Rk : Contact resistance (torch-electrode wire)
V_0 : Voltage of the no-load welding torch
L : Inductance of the welding throttle-arc current
Ve : Voltage drop on the electrode stickout
Va : Arc voltage drop
le : Wire extension

la   : Arc length

l   : Distance between the torch tip and the workpiece

Vm   : Melting speed of the electrode wire

Vf   : Speed of electrode wire feed

J   : Arc current density

de   : Electrode wire diameter

α i, β i and γ i   : Welding process constants.

Fig. 1   Electric circuit of MAG welding process

Equation(1) results from the electric circuit of the MAG-welding process (**Fig. 1**). Equation(2) results from the voltage of the wire extension. Equation(3) results from the characteristics of the MAG-welding process. Equation(4) results from melting speed of the wire. Equation(5) results from the physics of the MAG-welding process. Equation(6) corresponds to the estimation of current density.

The connection of arc length and wire extension is shown in **Fig. 2**. Equations(7), (8) can be deduced by the geometric condition of workpiece.

$$la_L = | A_L \cdot x + B_L(l-le) + C_L | /(A_L^2 + B_L^2)^{1/2} \quad (7)$$
$$la_R = | A_R \cdot x + B_R(l-le) + C_R | /(A_R^2 + B_R^2)^{1/2} \quad (8)$$

where

$A_L = -y_3$, $B_L = x_3 - x_1$, $C_L = x_1 \cdot y_3$, $AR = -y_4$, $B_R = x_4 - x_2$, $C_R = x_2 \cdot y_4$.

When welding process is with waving, the level locus of wire tip is

$$x = W/2 \cdot \sin(2 \cdot \pi \cdot f \cdot t) + d \quad (9)$$

where W, f is the width and frequency of weaving, t is time and d is shift from the center of weaving to groove.

As a result of a number of transformations, the following system of two states, non-linear simultaneous differential equations, is deduced by the system of equations(1)-(9) as follows:

When x < 0 (Arc is generated on the left side of the groove);

$$L \cdot dIa/dt = V_0 - \beta_2 - \beta_4 \cdot (A_L \cdot x + B_L \cdot l + C_L)/(A_L^2 + B_L^2)^{1/2}$$
$$- \{ R + \beta_1 + \beta_3 \cdot (A_L \cdot x + B_L \cdot l + C_L)/(A_L^2 + B_L^2)^{1/2} \} \cdot Ia$$
$$+ \beta_4 \cdot B_L \cdot le/(A_L^2 + B_L^2)^{1/2} + \{ \beta_3 \cdot B_L/(A_L^2 + B_L^2)1/2$$
$$- 4 \cdot \alpha_1/(\pi \cdot de^2) \} \cdot le \cdot Ia - \alpha_2 \cdot Vf \cdot \pi \cdot de^2/(4 \cdot Ia) \quad (10)$$

and when x > 0 (Arc is generated on the right side of the groove);

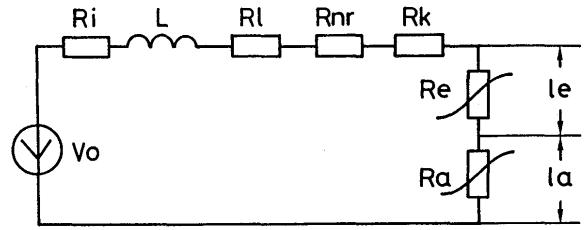$$L \cdot dIa/dt = V_0 - \beta_2 - \beta_4 \cdot (A_R \cdot x + B_R \cdot l + C_R)/(A_R^2 + B_R^2)^{1/2}$$
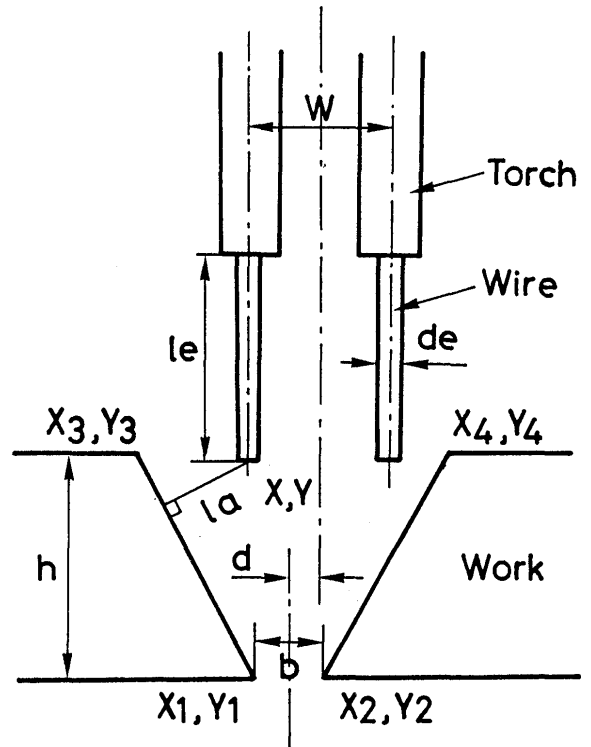

Fig. 2   Moving position of torch and geometry size of workpiece

$$- \{ R + \beta_1 + \beta_3 \cdot (A_R \cdot x + B_R \cdot l + C_R)/(A_R^2 + B_R^2)^{1/2} \} \cdot Ia$$
$$+ \beta_4 \cdot B_R \cdot le/(A_R^2 + B_R^2)^{1/2} + \{ \beta_3 \cdot B_R/(A_R^2 + B_R^2)^{1/2}$$
$$- 4 \cdot \alpha_1/(\pi \cdot de^2) \} \cdot le \cdot Ia - \alpha_2 Vf \cdot \pi \cdot de^2/(4 \cdot Ia) \quad (10')$$

$$dle/dt = Vf - 4 \cdot \gamma_1 \cdot Ia/(\pi \cdot de^2) - 16 \cdot \gamma_2/(\pi^2 \cdot de^4) \quad (11)$$

2.2 Results of calculation

To solve the above systems with the appropriate boundary conditions and the initial conditions, the following assumptions are made:

(1) welding occurs without short circuit in the arc gap

(2) noise components of arc current, arc voltage, sliding contact resistance and others are absent in the model.

(3) the process of metal transfer from the electrode

to the welding pool and filling in the grooving are not reflected in the model.

(4) welding arc occurs between the shortest distance from the wire tip to groove side of workpiece.

The given system of equations was solved with the help of Runge-Kutta's method. The following values were taken for the parameters in the equations(10) or (10'), (11)[2,3].

$R=0.01\,\Omega$, $L=0.001H$ $V_0=36V$, $Vf=215mm/sec$, $1=25mm$, $de=1.2mm$, $\alpha_1=0.001$, $\alpha_2=4.5$, $\beta_1=0.01$, $\beta_2=5.3$, $\beta_3=0.002$, $\beta_4=1.0$, $\gamma_1=0.01$, $\gamma_2=0.0012$.

The values of the parameters αi, βi, γi are taken on condition and method of welding with MAG.

In the **Fig . 2** the geometry size of workpiece are

$x_1=-1$ mm, $x_2=1$ mm, $x_3=-8$ mm, $x_4=8$ mm, $y_1=y_2=0$ mm, $y_3=y_4=16$ mm,

and initial condition of the welding process are[4,5,6]

$Ia=300$ A, $le=25mm$, $la=5mm$, $Va=30V$, $Ve=3V$, $W=5mm$.

When d = 1mm and h = 1Hz, its calculated result is shown in **Fig. 3**. Where Fig. 3(a) shows locus of wire tip in groove and Fig. 3(b) shows the current value corresponding to the locus of wire tip. After the current on the left(L) or right(R) is separately integrated with respect to time, the current differences between both can be calculated. Arc sensor modifies the shift between the torch to groove by detecting this current difference.

To observe the detecting sensitivity of arc sensor at difference frequencies, let $d=1$ mm and $h=1, 2\cdots6$ Hz. their current differences are shown in **Fig. 4**. It can be seen that with increase of weaving frequency, the current difference become large.
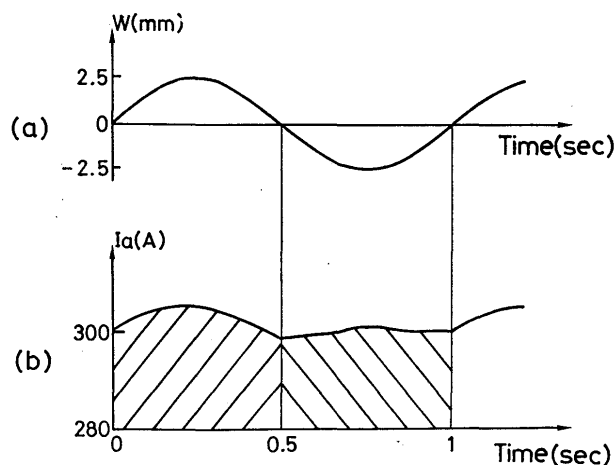
3. Experiments

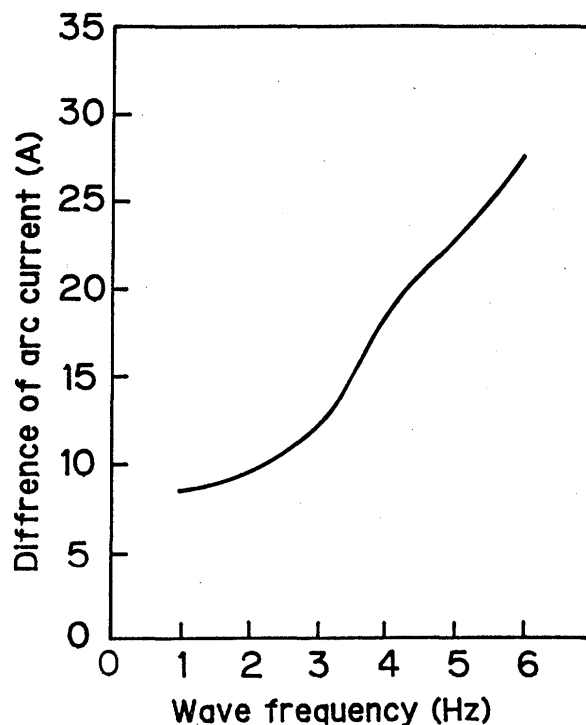Fig. 3   Result of calculation

Fig. 4   Relation between calculating current and frequency

3.1 Welding condition and detecting system

These experiments were carried out with a welding robot. Welding conditions agreed with the above used in the calculation, the shift from torch to groove is adjusted to 1 mm (d = 1mm), and the workpiece for experiment is made according to size in Fig. 2.

The circuit of system of detecting signal is shown in **Fig. 5**. To detect the welding current signal and torch position at the same time, A/D converter and U/D recorder are used in the circuit, The A/D converter is for detecting current signals in the welding process, The U/D recorder detects torch position by counting the pulse from the torch motor of the robot. The sampling-data of this system is 125/sec. After the signals are managed by the personal computer, it is possible that the results are directly graphed on to the display and saved in floppy disk for next using.

3.2 Experimental result

Fig. 6 shows the experimental results under H = 1Hz, Fig. 6(a) shows the locus of wave wire, Fig. 6(b) shows current value correspond to locus of wire tip. By using the method similar to that above, the current on left(L) or right(R) can be separately integrated with respect to time, the current difference of both sides can be calculated. **Fig. 7** shows the current difference under $H=1, 2\cdots6$ Hz. It is thus seen that the experimental results are distributed
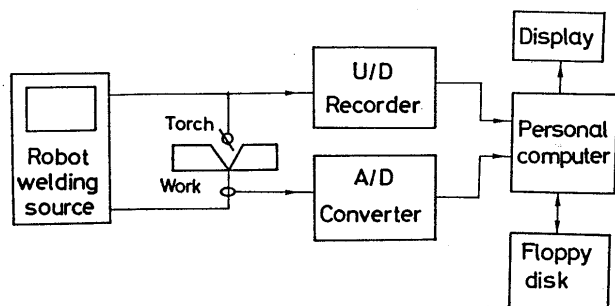
Fig. 5   Detecting system of experiment

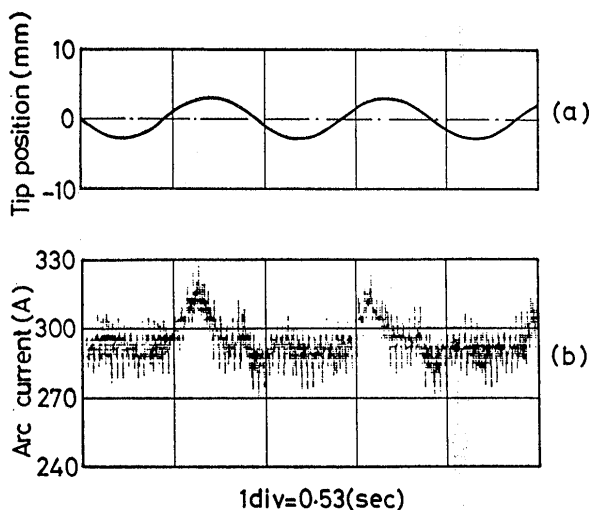1div=0·53(sec)

Fig. 6   Result of experiment

Fig. 7   Relation between experiment current and frequency

Fig. 8   Arc length of calculation of 1Hz and 6Hz

around a curve of calculations. Since the results of calculation and experiments are similar, the simultaneous differential equation deduced from theory and experiment are applicable in unstable welding process.

4. Discussion

Under differential frequency the arc length of each position in the groove can be calculated by (10), (10') and (11) equations. **Fig. 8** shows arc lengths of a period, Fig. 8(a) is of 1Hz, Fig. 8(b) is of 6Hz. Because the arc length of 6Hz is shorter than 1Hz, the current difference under high frequency is larger than low frequency. In practice, as the inductance exist in the circuit of the welding, when weaving becomes faster, the response of the arc self-regulation characteristics can not be expected to be so fast, as the arc length becomes shorter, the arc current difference becomes larger, the signal is detected easily. it is thus reason that the detecting sensitivity of the arc sensor is greatly influenced with the wave frequency of wire.

References

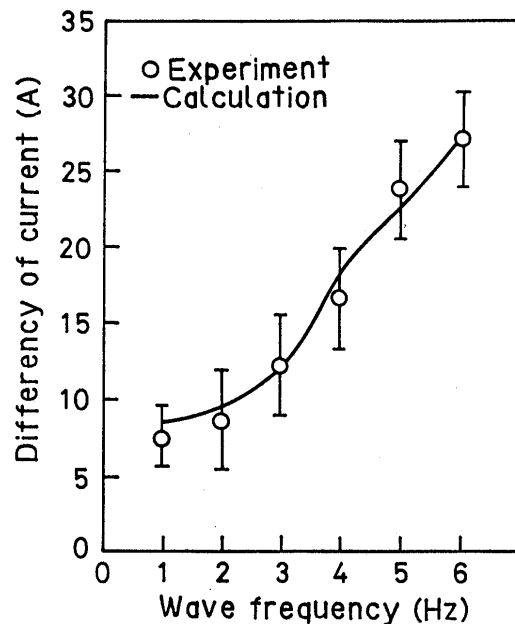1) J. E. Agapakis, N. Wittels and K. masubuchi; Automated Visual Weld Inspection for Robotic Welding Fabrication; Welding Automatic Control, No. 13, p. 143.

2) Y. Arata, K. Inoue; Application of Digital Computer to Pattern Measurement and Processing in Automatic Control System of Welding; J. JWS, Vol. 46, No. 3(1977), p. 129.(in Japanese)

3) J. -W. KIM and S. -J NA; A study on an Arc Sensor for Gas Metal Arc Welding of Horizontal Fillets; Welding Research Supplement, 216-s August 1991

4) H. Maruo, Y. Hirata; Wire Melting Speed in Pulsed MIG Welding; J.JWS, Vol. 3, No. 1(1985), p. 191.(in Japanese)

5) H. Maruo, Y. Hirata; Heat Contents and Temperature of Metal Droplets in Pulsed MIG Welding; J. JWS, Vol. 2, No. 4(1984), p. 573.(in Japanese)

6) J. Matsumoto, R Obata; Current-Voltage Characteristics for a Probe inserted in a Zone Surrounding the Welding Arc Column; J. JWS, Vol. 47, No. 11(1978), p. 753.(in Japanese)